Chapter 24

Intermittency

Sometimes They Come Back
—Stephen King

(R. Artuso, P. Dahlqvist, G. Tanner and P. Cvitanović)

I N THE THEORY of chaotic dynamics developed so far we assumed that the evolution operators have discrete spectra $\{z_0, z_1, z_2, \ldots\}$ given by the zeros of

$$1/\zeta(z) = (\cdots) \prod_k (1 - z/z_k).$$

The assumption was based on the tacit premise that the dynamics is everywhere exponentially unstable. Real life is nothing like that - state spaces are generically infinitely interwoven patterns of stable and unstable behaviors. The stable (in the case of Hamiltonian flows, integrable) orbits do not communicate with the ergodic components of the phase space, and can be treated by classical methods. In general, one is able to treat the dynamics near stable orbits as well as chaotic components of the phase space dynamics well within a periodic orbit approach. Problems occur at the borderline between chaos and regular dynamics where marginally stable orbits and manifolds present difficulties and still unresolved challenges.

We shall use the simplest example of such behavior - intermittency in 1-dimensional maps - to illustrate effects of marginal stability. The main message will be that spectra of evolution operators are no longer discrete, dynamical zeta functions exhibit branch cuts of the form

$$1/\zeta(z) = (\cdots) + (1 - z)^\alpha (\cdots),$$

and correlations decay no longer exponentially, but as power laws.
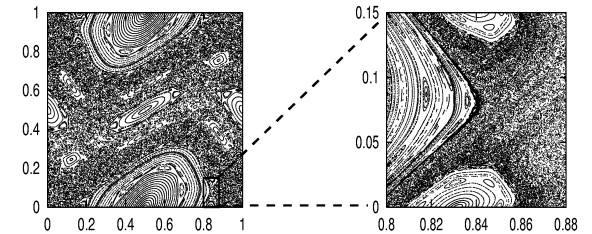
Figure 24.1: Typical phase space for an area-preserving map with mixed phase space dynamics; here the standard map for $k = 1.2$.

24.1 Intermittency everywhere

In many fluid dynamics experiments one observes transitions from regular behaviors to behaviors where long time intervals of regular behavior ("laminar phases") are interrupted by fast irregular bursts. The closer the parameter is to the onset of such bursts, the longer are the intervals of regular behavior. The distributions of laminar phase intervals are well described by power laws.

This phenomenon is called *intermittency*, and it is a very general aspect of dynamics, a shadow cast by non-hyperbolic, marginally stable state space regions. Complete hyperbolicity assumed in (18.5) is the exception rather than the rule, and for almost any dynamical system of interest (dynamics in smooth potentials, billiards with smooth walls, the infinite horizon Lorentz gas, etc.) one encounters mixed state spaces with islands of stability coexisting with hyperbolic regions, see figure 24.1 and example 7.7. Wherever stable islands are interspersed with chaotic regions, trajectories which come close to the stable islands can stay 'glued' for arbitrarily long times. These intervals of regular motion are interrupted by irregular bursts as the trajectory is re-injected into the chaotic part of the phase space. How the trajectories are precisely 'glued' to the marginally stable region is often hard to describe. What coarsely looks like a border of an island will under magnification dissolve into infinities of island chains of decreasing sizes, broken tori and bifurcating orbits, as illustrated in figure 24.1.

Intermittency is due to the existence of fixed points and cycles of marginal stability (5.6), or (in studies of the onset of intermittency) to the proximity of a nearly marginal complex or unstable orbits. In Hamiltonian systems intermittency goes hand in hand with the existence of (marginally stable) KAM tori. In more general settings, the existence of marginal or nearly marginal orbits is due to incomplete intersections of stable and unstable manifolds in a Smale horseshoe type dynamics (see figure 12.11). Following the stretching and folding of the invariant manifolds in time one will inevitably find state space points at which the stable and unstable manifolds are almost or exactly tangential to each other, implying nonexponential separation of nearby points in state space or, in other words, marginal stability. Under small parameter perturbations such neighborhoods undergo tangent bifurcations - a stable/unstable pair of periodic orbits is destroyed or created by coalescing into a marginal orbit, so the pruning which we shall encounter in chapter 12, and the intermittency discussed here are two sides of the same coin.
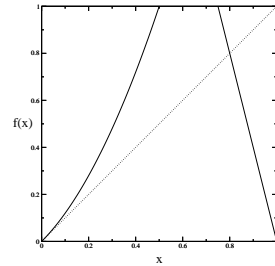
section 12.4

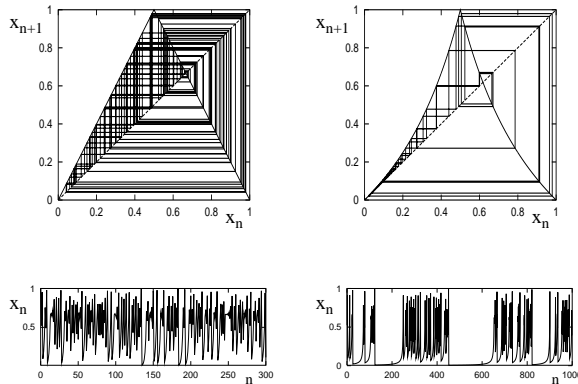**Figure 24.2:** A complete binary repeller with a marginal fixed point.

Figure 24.3: (a) A tent map trajectory. (b) A Farey map trajectory.

How to deal with the full complexity of a typical Hamiltonian system with mixed phase space is a very difficult, still open problem. Nevertheless, it is possible to learn quite a bit about intermittency by considering rather simple examples. Here we shall restrict our considerations to 1-dimensional maps which in the neighborhood of a single marginally stable fixed point at $x=0$ take the form

$$x \mapsto f(x) = x + O(x^{1+s}), \tag{24.1}$$

and are expanding everywhere else. Such a map may allow for escape, like the map shown in figure 24.2 or the dynamics may be bounded, like the Farey map

$$x \mapsto f(x) = \begin{cases} x/(1-x) & x \in [0, 1/2[\\ (1-x)/x & x \in [1/2, 1] \end{cases} \tag{24.2}$$

Figure 24.3 compares a trajectory of the tent map (11.4) side by side with a trajectory of the Farey map. In a stark contrast to the uniformly chaotic trajectory of the tent map, the Farey map trajectory alternates intermittently between slow regular motion close to the marginally stable fixed point, and chaotic bursts.   section 24.3.4

The presence of marginal stability has striking dynamical consequences: correlation decay may exhibit long range power law asymptotic behavior and diffusion processes can assume anomalous character. Escape from a repeller of the form figure 24.2 may be algebraic rather than exponential. In long time explorations of the dynamics intermittency manifests itself by enhancement of natural measure in the proximity of marginally stable cycles.

The questions we shall address here are: how does marginal stability affect zeta functions or spectral determinants? And, can we deduce power law decays of correlations from cycle expansions?

In example 23.5 we saw that marginal stability violates one of the conditions which ensure that the spectral determinant is an entire function. Already the simple fact that the cycle weight $1/|1 - \Lambda_p^r|$ in the trace (18.3) or the spectral determinant (19.3) diverges for marginal orbits with $|\Lambda_p| = 1$ tells us that we have to treat these orbits with care.

In the following we will incorporate marginal stability orbits into cycle-expansions in a systematic manner. To get to know the difficulties lying ahead, we will start in sect. 24.2 with a piecewise linear map, with the asymptotics (24.1). We will construct a dynamical zeta function in the usual way without worrying too much about its justification and show that it has a branch cut singularity. We will calculate the rate of escape from our piecewise linear map and find that it is characterized by decay, rather than exponential decay, a power law. We will show that dynamical zeta functions in the presence of marginal stability can still be written in terms of periodic orbits, exactly as in chapters 17 and 22, with one exception: the marginally stable orbits have to be explicitly excluded. This innocent looking step has far reaching consequences; it forces us to change the symbolic dynamics from a finite to an infinite alphabet, and entails a reorganization of the order of summations in cycle expansions, sect. 24.2.4.

Branch cuts are typical also for smooth intermittent maps with isolated marginally stable fixed points and cycles. In sect. 24.3, we discuss the cycle expansions and curvature combinations for zeta functions of smooth maps tailored to intermittency. The knowledge of the type of singularity one encounters enables us to develop the efficient resummation method presented in sect. 24.3.1.

Finally, in sect. 24.4, we discuss a probabilistic approach to intermittency that yields approximate dynamical zeta functions and provides valuable information about more complicated systems, such as billiards.

24.2 Intermittency for pedestrians

Intermittency does not only present us with a large repertoire of interesting dynamics, it is also at the root of many sorrows such as slow convergence of cycle expansions. In order to get to know the kind of problems which arise when studying dynamical zeta functions in the presence of marginal stability we will consider
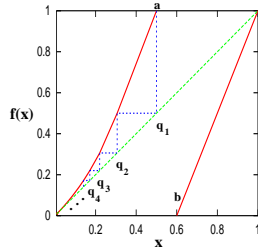
Figure 24.4: A piecewise linear intermittent map of (24.3) type: more specifically, the map piecewise linear over intervals (24.9) of the toy example studied below, $a = .5$, $b = .6$, $s = 1.0$.

an artfully concocted piecewise linear model first. From there we will move on to the more general case of smooth intermittant maps, sect. 24.3.

24.2.1 A toy map

The Bernoulli shift map (23.6) is an idealized, but highly instructive, example of a hyperbolic map. To study intermittency we will now construct a likewise piecewise linear model, an intermittent map stripped down to its bare essentials.

Consider a map $x \mapsto f(x)$ on the unit interval $\mathcal{M} = [0, 1]$ with two monotone branches

$$f(x) = \begin{cases} f_0(x) & \text{for } x \in \mathcal{M}_0 = [0, a] \\ f_1(x) & \text{for } x \in \mathcal{M}_1 = [b, 1] \end{cases} . \qquad (24.3)$$

The two branches are assumed complete, that is $f_0(\mathcal{M}_0) = f_1(\mathcal{M}_1) = \mathcal{M}$. The map allows escape if $a < b$ and is bounded if $a = b$ (see figure 24.2 and figure 24.4). We take the right branch to be expanding and linear:

$$f_1(x) = \frac{1}{1-b}(x - b) .$$

Next, we will construct the left branch in a way, which will allow us to model the intermittent behavior (24.1) near the origin. We chose a monotonically decreasing sequence of points q_n in $[0, a]$ with $q_1 = a$ and $q_n \to 0$ as $n \to \infty$. This sequence defines a partition of the left interval $\mathcal{M}_0$ into an infinite number of connected intervals $\mathcal{M}_n$, $n \geq 2$ with

$$\mathcal{M}_n =]q_n, q_{n-1}] \qquad \text{and} \qquad \mathcal{M}_0 = \bigcup_{n=2}^{\infty} \mathcal{M}_n. \qquad (24.4)$$

The map $f_0(x)$ is now specified by the following requirements

- $f_0(x)$ is continuous.

- $f_0(x)$ is linear on the intervals $\mathcal{M}_n$ for $n \geq 2$.

- $f_0(q_n) = q_{n-1}$, that is $\mathcal{M}_n = f_0^{-n+1}([a, 1])$.

This fixes the map for any given sequence $\{q_n\}$. The last condition ensures the existence of a simple Markov partition. The slopes of the various linear segments are

$$\begin{aligned} f_0'(x) &= \frac{f_0(q_{n-1}) - f_0(q_n)}{q_{n-1} - q_n} &= \frac{|\mathcal{M}_{n-1}|}{|\mathcal{M}_n|} && \text{for } x \in \mathcal{M}_n, \ n \geq 3 \\ f_0'(x) &= \frac{f_0(q_1) - f_0(q_2)}{q_1 - q_2} &= \frac{1-a}{|\mathcal{M}_2|} && \text{for } x \in \mathcal{M}_2 \\ f_0'(x) &= \frac{1}{1-b} &= \frac{|\mathcal{M}|}{|\mathcal{M}_1|} && \text{for } x \in \mathcal{M}_1 \end{aligned} \qquad (24.5)$$

with $|\mathcal{M}_n| = q_{n-1} - q_n$ for $n \geq 2$. Note that we do not require as yet that the map exhibit intermittent behavior.

We will see that the family of periodic orbits with code 10^n plays a key role for intermittent maps of the form (24.1). An orbit 10^n enters the intervals $\mathcal{M}_1 \to \mathcal{M}_{n+1} \to \mathcal{M}_n \to \ldots \to \mathcal{M}_2$ successively and the family approaches the marginal stable fixed point at $x = 0$ for $n \to \infty$. The stability of a cycle 10^n for $n \geq 1$ is given by the chain rule (4.46),

$$\Lambda_{10^n} = f_0'(x_{n+1})f_0'(x_n) \ldots f_0'(x_2)f_1'(x_1) = \frac{1}{|\mathcal{M}_{n+1}|} \frac{1-a}{1-b}, \qquad (24.6)$$

with $x_i \in \mathcal{M}_i$.

The properties of the map (24.3) are completely determined by the sequence $\{q_n\}$. By choosing $q_n = 2^{-n}$, for example, we recover the uniformly hyperbolic Bernoulli shift map (23.6). An intermittent map of the form (24.4) having the asymptotic behavior (24.1) can be constructed by choosing an algebraically decaying sequence $\{q_n\}$ behaving asymptotically like

$$q_n \sim \frac{1}{n^{1/s}}, \qquad (24.7)$$

where s is the intermittency exponent in (24.1). Such a partition leads to intervals whose length decreases asymptotically like a power-law, that is,

$$|\mathcal{M}_n| \sim \frac{1}{n^{1+1/s}} . \qquad (24.8)$$

As can be seen from (24.6), the Floquet multipliers of periodic orbit families approaching the marginal fixed point, such as the 10^n family increase in turn only algebraically with the cycle length.

It may now seem natural to construct an intermittent toy map in terms of a partition $|\mathcal{M}_n| = 1/n^{1+1/s}$, that is, a partition which follows (24.8) exactly. Such

a choice leads to a dynamical zeta function which can be written in terms of so-called Jonquière functions (or polylogarithms) which arise naturally also in the context of the Farey map (24.2), and the anomalous diffusion of sect. 25.3. We will, however, not go along this route here; instead, we will engage in a bit of reverse engineering and construct a less obvious partition which will simplify the algebra considerably later without loosing any of the key features typical for intermittent systems. We fix the intermittent toy map by specifying the intervals $\mathcal{M}_n$ in terms of Gamma functions according to

$$|\mathcal{M}_n| = C \frac{\Gamma(n+m-1/s-1)}{\Gamma(n+m)} \qquad \text{for} \quad n \geq 2, \tag{24.9}$$

where $m = [1/s]$ denotes the integer part of $1/s$ and C is a normalization constant fixed by the condition $\sum_{n=2}^{\infty} |\mathcal{M}_n| = q_1 = a$, that is,

$$C = a \left[\sum_{n=m+1}^{\infty} \frac{\Gamma(n-1/s)}{\Gamma(n+1)} \right]^{-1}. \tag{24.10}$$

Using Stirling's formula for the Gamma function

$$\Gamma(z) \sim e^{-z} z^{z-1/2} \sqrt{2\pi} \, (1 + 1/12z + \ldots),$$

we verify that the intervals decay asymptotically like $n^{-(1+1/s)}$, as required by the condition (24.8).

Next, let us write down the dynamical zeta function of the toy map in terms of its periodic orbits, that is

$$1/\zeta(z) = \prod_p \left(1 - \frac{z^{n_p}}{|\Lambda_p|} \right)$$

One may be tempted to expand the dynamical zeta function in terms of the binary symbolic dynamics of the map; we saw, however, in sect. 20.6 that such cycle expansion converges extremely slowly. The shadowing mechanism between orbits and pseudo-orbits fails for orbits of the form 10^n with stabilities given by (24.6), due to the marginal stability of the fixed point $\overline{0}$. It is therefore advantageous to choose as the fundamental cycles the family of orbits with code 10^n or, equivalently, switch from the finite (binary) alphabet to an infinite alphabet given by

$$10^{n-1} \to n.$$

Due to the piecewise-linear form of the map which maps intervals $\mathcal{M}_n$ exactly onto $\mathcal{M}_{n-1}$, all periodic orbits entering the left branch at least twice are canceled

exactly by pseudo cycles, and the cycle expanded dynamical zeta function depends only on the fundamental series $1, 10, 100, \ldots$:

$$
\begin{aligned}
1/\zeta(z) &= \prod_{p \neq 0} \left(1 - \frac{z^{n_p}}{|\Lambda_p|} \right) = 1 - \sum_{n=1}^{\infty} \frac{z^n}{|\Lambda_{10^{n-1}}|} \\
&= 1 - (1-b)z - C \frac{1-b}{1-a} \sum_{n=2}^{\infty} \frac{\Gamma(n+m-1/s-1)}{\Gamma(n+m)} z^n.
\end{aligned} \tag{24.11}
$$

The fundamental term (20.7) consists here of an infinite sum over algebraically decaying cycle weights. The sum is divergent for $|z| \geq 1$. We will see that this behavior is due to a branch cut of $1/\zeta$ starting at $z = 1$. We need to find analytic continuations of sums over algebraically decreasing terms in (24.11). Note also that we omitted the fixed point $\overline{0}$ in the above Euler product; we will discussed this point as well as a proper derivation of the zeta function in more detail in sect. 24.2.4.

24.2.2 Branch cuts

Starting from the dynamical zeta function (24.11), we first have to worry about finding an analytical continuation of the sum for $|z| \geq 1$. We do, however, get this part for free here due to the particular choice of interval lengths made in (24.9). The sum over ratios of Gamma functions in (24.11) can be evaluated analytically by using the following identities valid for $1/s = \alpha > 0$ (the famed binomial theorem in disguise),

- α non-integer

$$(1-z)^\alpha = \sum_{n=0}^{\infty} \frac{\Gamma(n-\alpha)}{\Gamma(-\alpha)\Gamma(n+1)} z^n \tag{24.12}$$

- α integer

$$
\begin{aligned}
(1-z)^\alpha \log(1-z) &= \sum_{n=1}^{\alpha} (-1)^n c_n z^n \\
&\quad + (-1)^{\alpha+1} \alpha! \sum_{n=\alpha+1}^{\infty} \frac{(n-\alpha-1)!}{n!} z^n
\end{aligned} \tag{24.13}
$$

with

$$c_n = \binom{\alpha}{n} \sum_{k=0}^{n-1} \frac{1}{\alpha-k}.$$

In order to simplify the notation, we restrict the intermittency parameter to the range $1 \le 1/s < 2$ with $[1/s] = m = 1$. All what follows can easily be generalized to arbitrary $s > 0$ using equations (24.12) and (24.13). The infinite sum in (24.11) can now be evaluated with the help of (24.12) or (24.13), that is,

$$\sum_{n=2}^{\infty} \frac{\Gamma(n - 1/s)}{\Gamma(n+1)} z^n = \begin{cases} \Gamma(-\frac{1}{s})\left[(1-z)^{1/s} - 1 + \frac{1}{s}z\right] & \text{for} \quad 1 < 1/s < 2; \\ (1-z)\log(1-z) + z & \text{for} \quad s = 1 . \end{cases}$$

The normalization constant C in (24.9) can be evaluated explicitly using (24.10) and the dynamical zeta function can be given in closed form. We obtain for $1 < 1/s < 2$

$$1/\zeta(z) = 1 - (1-b)z - \frac{a}{1/s - 1}\frac{1-b}{1-a}\left((1-z)^{1/s} - 1 + \frac{1}{s}z\right). \qquad (24.14)$$

and for $s = 1$,

$$1/\zeta(z) = 1 - (1-b)z - a\frac{1-b}{1-a}\left((1-z)\log(1-z) + z\right). \qquad (24.15)$$

It now becomes clear why the particular choice of intervals $\mathcal{M}_n$ made in the last section is useful; by summing over the infinite family of periodic orbits 0^n1 explicitly, we have found the desired analytical continuation for the dynamical zeta function for $|z| \ge 1$. The function has a branch cut starting at the branch point $z = 1$ and running along the positive real axis. That means, the dynamical zeta function takes on different values when approaching the positive real axis for $\mathrm{Re}\, z > 1$ from above and below. The dynamical zeta function for general $s > 0$ takes on the form

$$1/\zeta(z) = 1 - (1-b)z - \frac{a}{g_s(1)}\frac{1-b}{1-a}\frac{1}{z^{m-1}}\left((1-z)^{1/s} - g_s(z)\right) \qquad (24.16)$$

for non-integer s with $m = [1/s]$ and

$$1/\zeta(z) = 1 - (1-b)z - \frac{a}{g_m(1)}\frac{1-b}{1-a}\frac{1}{z^{m-1}}\left((1-z)^m \log(1-z) - g_m(z)\right) (24.17)$$

for $1/s = m$ integer and $g_s(z)$ are polynomials of order $m = [1/s]$ which can be deduced from (24.12) or (24.13). We thus find algebraic branch cuts for non integer intermittency exponents $1/s$ and logarithmic branch cuts for $1/s$ integer. We will see in sect. 24.3 that branch cuts of that form are generic for 1-dimensional intermittent maps.

Branch cuts are the all important new feature of dynamical zeta functions due to intermittency. So, how do we calculate averages or escape rates of the dynamics of the map from a dynamical zeta function with branch cuts? We take 'a learning by doing' approach and calculate the escape from our toy map for $a < b$.

Figure 24.5: The survival probability Γ_n calculated by contour integration; integrating (24.18) inside the domain of convergence $|z| < 1$ (shaded area) of $1/\zeta(z)$ in periodic orbit representation yields (18.26). A deformation of the contour γ_r^- (dashed line) to a larger circle γ_R^- gives contributions from the poles and zeros (x) of $1/\zeta(z)$ between the two circles. These are the only contributions for hyperbolic maps (a), for intermittent systems additional contributions arise, given by the contour γ_{cut} running along the branch cut (b).

(a)   (b)
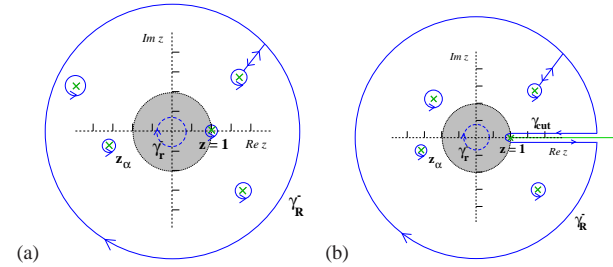
24.2.3 Escape rate

Our starting point for the calculation of the fraction of survivors after n time steps, is the integral representation (19.19)

$$\Gamma_n = \frac{1}{2\pi i}\oint_{\gamma_r^-} z^{-n}\left(\frac{d}{dz}\log \zeta^{-1}(z)\right)dz, \qquad (24.18)$$

where the contour encircles the origin in the clockwise direction. If the contour lies inside the unit circle $|z| = 1$, we may expand the logarithmic derivative of $\zeta^{-1}(z)$ as a convergent sum over all periodic orbits. Integrals and sums can be interchanged, the integrals can be solved term by term, and the formula (18.26) is recovered. For hyperbolic maps, cycle expansion methods or other techniques may provide an analytic extension of the dynamical zeta function beyond the leading zero; we may therefore deform the original contour into a larger circle with radius R which encircles both poles and zeros of $\zeta^{-1}(z)$, see figure 24.5 (a). Residue calculus turns this into a sum over the zeros z_α and poles z_β of the dynamical zeta function, that is

$$\Gamma_n = \sum_{|z_\alpha|<R}^{\text{zeros}} \frac{1}{z_\alpha^n} - \sum_{|z_\beta|<R}^{\text{poles}} \frac{1}{z_\beta^n} + \frac{1}{2\pi i}\oint_{\gamma_R^-} dz\, z^{-n}\frac{d}{dz}\log\zeta^{-1}, \qquad (24.19)$$

where the last term gives a contribution from a large circle γ_R^-. We thus find exponential decay of Γ_n dominated by the leading zero or pole of $\zeta^{-1}(z)$.

Things change considerably in the intermittent case. The point $z = 1$ is a branch cut singularity and there exists no Taylor series expansion of ζ^{-1} around $z = 1$. Second, the path deformation that led us to (24.19) requires more care, as it must not cross the branch cut. When expanding the contour to large $|z|$ values, we have to deform it along the branch $\mathrm{Re}\,(z) \ge 1$, $\mathrm{Im}\,(z) = 0$ encircling the branch cut in anti-clockwise direction, see figure 24.5 (b). We will denote the detour around the cut as γ_{cut}. We may write symbolically

$$\oint_{\gamma_r} = \sum^{\text{zeros}} - \sum^{\text{poles}} + \oint_{\gamma_R} + \oint_{\gamma_{cut}}$$

where the sums include only the zeros and the poles in the area enclosed by the contours. The asymptotics is controlled by the zero, pole or cut closest to the origin.

Let us now go back to our intermittent toy map. The asymptotics of the survival probability of the map is here governed by the behavior of the integrand $\frac{d}{dz} \log \zeta^{-1}$ in (24.18) at the branch point $z = 1$. We restrict ourselves again to the case $1 < 1/s < 2$ first and write the dynamical zeta function (24.14) in the form

$$1/\zeta(z) = a_0 + a_1(1 - z) + b_0(1 - z)^{1/s} \equiv G(1 - z)$$

and

$$a_0 = \frac{b - a}{1 - a}, \quad b_0 = \frac{a}{1 - 1/s}\frac{1 - b}{1 - a}.$$

Setting $u = 1 - z$, we need to evaluate

$$\frac{1}{2\pi i} \oint_{\gamma_{cut}} (1 - u)^{-n} \frac{d}{du} \log G(u) du \tag{24.20}$$

where γ_{cut} goes around the cut (i.e., the negative u axis). Expanding the integrand $\frac{d}{du} \log G(u) = G'(u)/G(u)$ in powers of u and $u^{1/s}$ at $u = 0$, one obtains

$$\frac{d}{du} \log G(u) = \frac{a_1}{a_0} + \frac{1}{s}\frac{b_0}{a_0} u^{1/s-1} + O(u). \tag{24.21}$$

The integrals along the cut may be evaluated using the general formula

$$\frac{1}{2\pi i} \oint_{\gamma_{cut}} u^\alpha (1 - u)^{-n} du = \frac{\Gamma(n - \alpha - 1)}{\Gamma(n)\Gamma(-\alpha)} \sim \frac{1}{n^{\alpha+1}}(1 + O(1/n)) \tag{24.22}$$

which can be obtained by deforming the contour back to a loop around the point $u = 1$, now in positive (anti-clockwise) direction. The contour integral then picks up the $(n-1)$st term in the Taylor expansion of the function u^α at $u = 1$, cf. (24.12). For the continuous time case the corresponding formula is

$$\frac{1}{2\pi i} \oint_{\gamma_{cut}} z^\alpha e^{zt} dz = \frac{1}{\Gamma(-\alpha)} \frac{1}{t^{\alpha+1}}. \tag{24.23}$$

Plugging (24.21) into (24.20) and using (24.22) we get the asymptotic result

$$\Gamma_n \sim \frac{b_0}{a_0}\frac{1}{s}\frac{1}{\Gamma(1 - 1/s)}\frac{1}{n^{1/s}} = \frac{a}{s - 1}\frac{1 - b}{b - a}\frac{1}{\Gamma(1 - 1/s)}\frac{1}{n^{1/s}}. \tag{24.24}$$
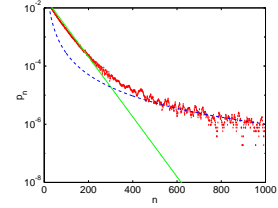
Figure 24.6: The asymptotic escape from an intermittent repeller is a power law. Normally it is preceded by an exponential, which can be related to zeros close to the cut but beyond the branch point $z = 1$, as in figure 24.5 (b).

We see that, asymptotically, the escape from an intermittent repeller is described by power law decay rather than the exponential decay we are familiar with for hyperbolic maps; a numerical simulation of the power-law escape from an intermittent repeller is shown in figure 24.6.

For general non-integer $1/s > 0$, we write

$$1/\zeta(z) = A(u) + (u)^{1/s} B(u) \equiv G(u)$$

with $u = 1 - z$ and $A(u)$, $B(u)$ are functions analytic in a disc of radius 1 around $u = 0$. The leading terms in the Taylor series expansions of $A(u)$ and $B(u)$ are

$$a_0 = \frac{b - a}{1 - a}, \quad b_0 = \frac{a}{g_s(1)}\frac{1 - b}{1 - a},$$

see (24.16). Expanding $\frac{d}{du} \log G(u)$ around $u = 0$, one again obtains leading order contributions according to (24.21) and the general result follows immediately using (24.22), that is,

$$\Gamma_n \sim \frac{a}{s g_s(1)}\frac{1 - b}{b - a}\frac{1}{\Gamma(1 - 1/s)}\frac{1}{n^{1/s}}. \tag{24.25}$$

Applying the same arguments for integer intermittency exponents $1/s = m$, one obtains

$$\Gamma_n \sim (-1)^{m+1}\frac{a}{s g_m(1)}\frac{1 - b}{b - a}\frac{m!}{n^m}. \tag{24.26}$$

So far, we have considered the survival probability for a repeller, that is we assumed $a < b$. The formulas (24.25) and (24.26) do obviously not apply for the case $a = b$, that is, for the bounded map. The coefficient $a_0 = (b - a)/(1 - a)$ in the series representation of $G(u)$ is zero, and the expansion of the logarithmic derivative of $G(u)$ (24.21) is no longer valid. We get instead

$$\frac{d}{du} \log G(u) = \begin{cases} \frac{1}{u}\left(1 + O(u^{1/s-1})\right) & s < 1 \\ \frac{1}{u}\left(\frac{1}{s} + O(u^{1-1/s})\right) & s > 1 \end{cases},$$

assuming non-integer $1/s$ for convenience. One obtains for the survival probability.

$$\Gamma_n \sim \begin{cases} 1 + O(n^{1-1/s}) & s < 1 \\ 1/s + O(n^{1/s-1}) & s > 1 \end{cases} \ .$$

For $s > 1$, this is what we expect. There is no escape, so the survival probability is equal to 1, which we get as an asymptotic result here. The result for $s > 1$ is somewhat more worrying. It says that Γ_n defined as sum over the instabilities of the periodic orbits as in (22.18) does not tend to unity for large n. However, the case $s > 1$ is in many senses anomalous. For instance, the invariant density cannot be normalized. It is therefore not reasonable to expect that periodic orbit theories will work without complications.

24.2.4 Why does it work (anyway)?

Due to the piecewise linear nature of the map constructed in the previous section, we had the nice property that interval lengths did exactly coincide with the inverse of the stability of periodic orbits of the system, that is

$$|\mathcal{M}_n| = 1/|\Lambda_{10}|^{n-1}.$$

There is thus no problem in replacing the survival probability Γ_n given by (1.2), (22.2), that is the fraction of state space $\mathcal{M}$ surviving n iterations of the map,

$$\Gamma_n = \frac{1}{|\mathcal{M}|} \sum_i^{(n)} |\mathcal{M}_i|.$$

by a sum over periodic orbits of the form (18.26). The only orbit to worry about is the marginal fixed point $\overline{0}$ itself which we excluded from the zeta function (24.11).

For smooth intermittent maps, things are less clear and the fact that we had to prune the marginal fixed point is a warning sign that interval estimates by periodic orbit stabilities might go horribly wrong. The derivation of the survival probability in terms of cycle stabilities in chapter 22 did indeed rely heavily on a hyperbolicity assumption which is clearly not fulfilled for intermittent maps. We therefore have to carefully reconsider this derivation in order to show that periodic orbit formulas are actually valid for intermittent systems in the first place.

We will for simplicity consider maps, which have a finite number of say s branches defined on intervals $\mathcal{M}_s$ and we assume that the map maps each interval $\mathcal{M}_s$ onto $\mathcal{M}$, that is $f(\mathcal{M}_s) = \mathcal{M}$. This ensures the existence of a complete symbolic dynamics - just to make things easy (see figure 24.2).

The generating partition is composed of the domains $\mathcal{M}_s$. The nth level partition $C^{(n)} = \{\mathcal{M}_i\}$ can be constructed iteratively. Here i's are words $i = s_2 s_2 \ldots s_n$ of length n, and the intervals $\mathcal{M}_i$ are constructed recursively

$$\mathcal{M}_{sj} = f_s^{-1}(\mathcal{M}_j), \tag{24.27}$$

where sj is the concatenation of letter s with word j of length $n_j < n$.

In what follows we will concentrate on the survival probability Γ_n, postponing other quantities of interest, such as averages, to later considerations. In establishing the equivalence of the survival probability and the periodic orbit formula for the escape rate for hyperbolic systems we have assumed that the map is expanding, with a minimal expansion rate $|f'(x)| \geq \Lambda_{\min} > 1$. This enabled us to bound the size of every survivor strip $\mathcal{M}_i$ by (22.6), the stability Λ_i of the periodic orbit i within the $\mathcal{M}_i$, and bound the survival probability by the periodic orbit sum (22.7).

The bound (22.6)

$$C_1 \frac{1}{|\Lambda_i|} < \frac{|\mathcal{M}_i|}{|\mathcal{M}|} < C_2 \frac{1}{|\Lambda_i|}$$

relies on hyperbolicity, and is thus indeed violated for intermittent systems. The problem is that now there is no lower bound on the expansion rate, the minimal expansion rate is $\Lambda_{\min} = 1$. The survivor strip $\mathcal{M}_{0^n}$ which includes the marginal fixed point is thus completely overestimated by $1/|\Lambda_{0^n}| = 1$ which is constant for all n.

However, bounding survival probability strip by strip is not what is required for establishing the bound (22.7). For intermittent systems a somewhat weaker bound can be established, saying that the average size of intervals *along a periodic orbit* can be bounded close to the stability of the periodic orbit for all but the interval $\mathcal{M}_{0^n}$. The weaker bound applies to averaging over each prime cycle p separately

$$C_1 \frac{1}{|\Lambda_p|} < \frac{1}{n_p} \sum_{i \in p} \frac{|\mathcal{M}_i|}{|\mathcal{M}|} < C_2 \frac{1}{|\Lambda_p|}, \tag{24.28}$$

where the word i represents a code of the periodic orbit p and all its cyclic permutations. It can be shown that one can find positive constants C_1, C_2 independent of p. Summing over all periodic orbits leads then again to (22.7).

To study averages of multiplicative weights we follow sect. 17.1 and introduce a state space observable $a(x)$ and the integrated quantity

$$A^n(x) = \sum_{k=0}^{n-1} a(f^k(x)).$$

Figure 24.7: Transition graph corresponding to the alphabet $\{0^{k-1}1; \overline{0}, \ k \geq 1\}$
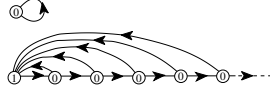
This leads us to introduce the generating function (17.10)

$$\langle e^{\beta \, A^n(x)} \rangle,$$

where $\langle . \rangle$ denote some averaging over the distribution of initial points, which we choose to be uniform (rather than the *a priori* unknown invariant density). Again, all we have to show is, that constants C_1, C_2 exist, such that

$$C_1 \frac{e^{\beta A_p}}{|\Lambda_p|} < \frac{1}{n_p} \sum_{i \in p} \frac{1}{|\mathcal{M}|} \int_{\mathcal{M}_Q} e^{\beta A^n(x)} dx < C_2 \frac{e^{\beta A_p}}{|\Lambda_p|}, \qquad (24.29)$$

is valid for all p. After performing the above average one gets

$$C_1 \Gamma_n(\beta) < \frac{1}{|\mathcal{M}|} \int_{\mathcal{M}} e^{\beta A(x,n)} dx < C_2 \Gamma_n(\beta), \qquad (24.30)$$

with

$$\Gamma_n(\beta) = \sum_p^n \frac{e^{\beta A_p}}{|\Lambda_p|}. \qquad (24.31)$$

and a dynamical zeta function can be derived. In the intermittent case one can expect that the bound (24.29) holds using an averaging argument similar to the one discussed in (24.28). This justifies the use of dynamical zeta functions for intermittent systems.

One lesson we should have learned so far is that the natural alphabet to use is not $\{0, 1\}$ but rather the infinite alphabet $\{0^{k-1}1, \overline{0}; \ k \geq 1\}$. The symbol 0 occurs unaccompanied by any 1's only in the $\overline{0}$ marginal fixed point which is disconnected from the rest of the transition graph, see figure 24.7.

What happens if we remove a single prime cycle from a dynamical zeta function? In the hyperbolic case such a removal introduces a pole in the $1/\zeta$ and slows down the convergence of cycle expansions. The heuristic interpretation of such a pole is that for a subshift of finite type removal of a single prime cycle leads to unbalancing of cancellations within the infinity of of shadowing pairs. Nevertheless, removal of a single prime cycle is an exponentially small perturbation of the trace sums, and the asymptotics of the associated trace formulas is unaffected.

In the intermittent case, the fixed point $\overline{0}$ does not provide any shadowing , and a statement such as

$$\Lambda_{1 \cdot 0^{k+1}} \approx \Lambda_{1 \cdot 0^k} \Lambda_0,$$

is meaningless. It seems therefore sensible to take out the factor $(1 - t_0) = 1 - z$ from the product representation of the dynamical zeta function (19.15), that is, to consider a pruned dynamical zeta function $1/\zeta_{inter}(z)$ defined by

$$1/\zeta(z) = (1 - z)1/\zeta_{inter}(z) \, .$$

We saw in the last sections, that the zeta function $1/\zeta_{inter}(z)$ has all the nice properties we know from the hyperbolic case, that is, we can find a cycle expansion with - in the toy model case - vanishing curvature contributions and we can calculate dynamical properties like escape after having understood, how to handle the branch cut. But you might still be worried about leaving out the extra factor $1 - z$ all together. It turns out, that this is not only a matter of convenience, omitting the marginal $\overline{0}$ cycle is a dire necessity. The cycle weight $\Lambda_0^n = 1$ overestimates the corresponding interval length of $\mathcal{M}_{0^n}$ in the partition of the state space $\mathcal{M}$ by an increasing amount thus leading to wrong results when calculating escape. By leaving out the $\overline{0}$ cycle (and thus also the $\mathcal{M}_{0^n}$ contribution), we are guaranteed to get at least the right asymptotical behavior.

Note also, that if we are working with the spectral determinant (19.3), given in product form as

$$\det(1 - z\mathcal{L}) = \prod_p \prod_{m=0}^{\infty} \left(1 - \frac{z^{n_p}}{|\Lambda_p| \Lambda_p^m}\right) \, ,$$

for intermittent maps the marginal stable cycle has to be excluded. It introduces an (unphysical) essential singularity at $z = 1$ due the presence of a factor $(1 - z)^{\infty}$ stemming from the $\overline{0}$ cycle.

24.3 Intermittency for cyclists

Admittedly, the toy map is what is says - a toy model. The piece wise linearity of the map led to exact cancellations of the curvature contributions leaving only the fundamental terms. There are still infinitely many orbits included in the fundamental term, but the cycle weights were chosen in such a way that the zeta function could be written in closed form. For a smooth intermittent map this all will not be the case in general; still, we will argue that we have already seen almost all the fundamentally new features due to intermittency. What remains are technicalities - not necessarily easy to handle, but nothing very surprise any more.

In the following we will sketch, how to make cycle expansion techniques work for general 1-dimensional maps with a single isolated marginal fixed point. To keep the notation simple, we will consider two-branch maps with a complete binary symbolic dynamics as for example the Farey map, figure 24.3, or the repeller depicted in figure 24.2. We again assume that the behavior near the fixed point is given by (24.1). This implies that the stability of a family of periodic orbits approaching the marginally stable orbit, as for example the family 10^n, will increase only algebraically, that is we find again for large n

$$\frac{1}{\Lambda_{10^n}} \sim \frac{1}{n^{1+1/s}},$$

where s denotes the intermittency exponent.

When considering zeta functions or trace formulas, we again have to take out the marginal orbit $\overline{0}$; periodic orbit contributions of the form t_{0^n1} are now unbalanced and we arrive at a cycle expansion in terms of infinitely many fundamental terms as for our toy map. This corresponds to moving from our binary symbolic dynamics to an infinite symbolic dynamics by making the identification

$$10^{n-1} \to n; \quad 10^{n-1}10^{m-1} \to nm; \quad 10^{n-1}10^{m-1}10^{k-1} \to nmk; \ldots$$

see also table 24.1. The topological length of the orbit is thus no longer determined by the iterations of our two-branch map, but by the number of times the cycle goes from the right to the left branch. Equivalently, one may define a new map, for which all the iterations on the left branch are done in one step. Such a map is called an *induced map* and the topological length of orbits in the infinite alphabet corresponds to the iterations of this induced map.

exercise 12.1

For generic intermittent maps, curvature contributions in the cycle expanded zeta function will not vanish exactly. The most natural way to organize the cycle expansion is to collect orbits and pseudo orbits of the same topological length with respect to the infinite alphabet. Denoting cycle weights in the new alphabet as $t_{nm\ldots} = t_{10^{n-1}10^{m-1}\ldots}$, one obtains

$$
\begin{aligned}
\zeta^{-1} &= \prod_{p\neq 0}\left(1 - t_p\right) = 1 - \sum_{n=1}^{\infty} ce \\
&= 1 - \sum_{n=1}^{\infty} t_n - \sum_{m=1}^{\infty}\sum_{n=1}^{\infty}\frac{1}{2}(t_{mn} - t_m t_n) \\
&\quad - \sum_{k=1}^{\infty}\sum_{m=1}^{\infty}\sum_{n=1}^{\infty}(\frac{1}{3}t_{kmn} - \frac{1}{2}t_{km}t_n + \frac{1}{6}t_k t_m t_n) - \sum_{l=1}^{\infty}\sum_{k=1}^{\infty}\sum_{m=1}^{\infty}\sum_{n=1}^{\infty}\cdots.
\end{aligned}
$$

(24.32)

The first sum is the fundamental term, which we have already seen in the toy model, (24.11). The curvature terms c_n in the expansion are now e-fold infinite sums where the prefactors take care of double counting of prime periodic orbits.

Table 24.1: Infinite alphabet versus the original binary alphabet for the shortest periodic orbit families. Repetitions of prime cycles ($11 = 1^2, 0101 = 01^2, \ldots$) and their cyclic repeats ($110 = 101, 1110 = 1101, \ldots$) are accounted for by cancelations and combination factors in the cycle expansion (24.32).

∞ – alphabet		binary alphabet				
		$n=1$	$n=2$	$n=3$	$n=4$	$n=5$
1-cycles	n	1	10	100	1000	10000
2-cycles	mn					
	$1n$	11	110	1100	11000	110000
	$2n$	101	0101	10100	101000	1010000
	$3n$	1001	10010	100100	1001000	10010000
	$4n$	10001	100010	1000100	10001000	100010000
3-cycles	kmn					
	$11n$	111	1110	11100	111000	1110000
	$12n$	1101	11010	110100	1101000	11010000
	$13n$	11001	110010	1100100	11001000	110010000
	$21n$	1011	10110	101100	1011000	10110000
	$22n$	10101	101010	1010100	10101000	101010000
	$23n$	101001	1010010	10100100	101001000	1010010000
	$31n$	10011	100110	1001100	10011000	100110000
	$32n$	100101	1001010	10010100	100101000	1001010000
	$33n$	1001001	10010010	100100100	1001001000	10010010000

Let us consider the fundamental term first. For generic intermittent maps, we can not expect to obtain an analytic expression for the infinite sum of the form

$$f(z) = \sum_{n=0}^{\infty} h_n z^n. \tag{24.33}$$

with algebraically decreasing coefficients

$$h_n \sim \frac{1}{n^\alpha} \quad \text{with} \quad \alpha > 0$$

To evaluate the sum, we face the same problem as for our toy map: the power series diverges for $z > 1$, that is, exactly in the 'interesting' region where poles, zeros or branch cuts of the zeta function are to be expected. By carefully subtracting the asymptotic behavior with the help of (24.12) or (24.13), one can in general construct an analytic continuation of $f(z)$ around $z = 1$ of the form

$$
\begin{aligned}
f(z) &\sim A(z) + (1-z)^{\alpha-1}B(z) & \alpha \notin \mathbb{N} \\
f(z) &\sim A(z) + (1-z)^{\alpha-1}\ln(1-z) & \alpha \in \mathbb{N},
\end{aligned}
\tag{24.34}
$$

where $A(z)$ and $B(z)$ are functions analytic in a disc around $z = 1$. We thus again find that the zeta function (24.32) has a branch cut along the real axis $\operatorname{Re} z \geq 1$.

From here on we can switch to auto-pilot and derive algebraic escape, decay of correlation and all the rest. We find in particular that the asymptotic behavior derived in (24.25) and (24.26) is a general result, that is, the survival probability is given asymptotically by

$$\Gamma_n \sim C\frac{1}{n^{1/s}} \tag{24.35}$$

for all 1-dimensional maps of the form (24.1). We have to work a bit harder if we want more detailed information like the prefactor C, exponential precursors given by zeros or poles of the dynamical zeta function or higher order corrections. This information is buried in the functions $A(z)$ and $B(z)$ or more generally in the analytically continued zeta function. To get this analytic continuation, one may follow either of the two different strategies which we will sketch next.

24.3.1   Resummation

One way to get information about the zeta function near the branch cut is to derive the leading coefficients in the Taylor series of the functions $A(z)$ and $B(z)$ in (24.34) at $z = 1$. This can be done in principle, if the coefficients h_n in sums like (24.33) are known (as for our toy model). One then considers a resummation of the form

$$\sum_{j=0}^{\infty} h_j z^j = \sum_{j=0}^{\infty} a_j(1-z)^j + (1-z)^{\alpha-1}\sum_{j=0}^{\infty} b_j(1-z)^j, \tag{24.36}$$

and the coefficients a_j and b_j are obtained in terms of the h_j's by expanding $(1-z)^j$ and $(1-z)^{j+\alpha-1}$ on the right hand side around $z = 0$ using (24.12) and equating the coefficients.

In practical calculations one often has only a finite number of coefficients h_j, $0 \leq j \leq N$, which may have been obtained by finding periodic orbits and their stabilities numerically. One can still design a resummation scheme for the computation of the coefficients a_j and b_j in (24.36). We replace the infinite sums in (24.36) by finite sums of increasing degrees n_a and n_b, and require that

$$\sum_{i=0}^{n_a} a_i(1-z)^i + (1-z)^{\alpha-1}\sum_{i=0}^{n_b} b_i(1-z)^i = \sum_{i=0}^{N} h_i z^i + O(z^{N+1}) \ . \tag{24.37}$$

One proceeds again by expanding the right hand side around $z = 0$, skipping all powers z^{N+1} and higher, and then equating coefficients. It is natural to require that $|n_b + \alpha - 1 - n_a| < 1$, so that the maximal powers of the two sums in (24.37) are adjacent. If one chooses $n_a + n_b + 2 = N + 1$, then, for each cutoff length N, the integers n_a and n_b are uniquely determined from a linear system of equations. The

price we pay is that the so obtained coefficients depend on the cutoff N. One can now study convergence of the coefficients a_j, and b_j, with respect to increasing values of N, or various quantities derived from a_j and b_j. Note that the leading coefficients a_0 and b_0 determine the prefactor C in (24.35), cf. (24.24). The re-summed expression can also be used to compute zeros, inside or outside the radius of convergence of the cycle expansion $\sum h_j z^j$.

The scheme outlined in this section tacitly assumes that a representation of form (24.34) holds in a disc of radius 1 around $z = 1$. Convergence is improved further if additional information about the asymptotics of sums like (24.33) is used to improve the ansatz (24.36).

24.3.2   Analytical continuation by integral transformations

We will now introduce a method which provides an analytic continuation of sums of the form (24.33) without explicitly relying on an ansatz (24.36). The main idea is to rewrite the sum (24.33) as a sum over integrals with the help of the Poisson summation formula and find an analytic continuation of each integral by contour deformation. In order to do so, we need to know the n dependence of the coefficients $h_n \equiv h(n)$ explicitly for all n. If the coefficients are not known analytically, one may proceed by approximating the large n behavior in the form

$$h(n) = n^{-\alpha}(C_1 + C_2 n^{-1} + \ldots), \qquad n \neq 0 \,,$$

and determine the constants C_i numerically from periodic orbit data. By using the Poisson resummation identity

$$\sum_{n=-\infty}^{\infty} \delta(x-n) = \sum_{m=-\infty}^{\infty} \exp(2\pi imx) \,, \tag{24.38}$$

we may write the sum as (24.33)

$$f(z) = \frac{1}{2}h(0) + \sum_{m=-\infty}^{\infty} \int_0^{\infty} dx\, e^{2\pi imx} h(x) z^x. \tag{24.39}$$

The continuous variable x corresponds to the discrete summation index n and it is convenient to write $z = r\exp(i\sigma)$ from now on. The integrals are still not convergent for $r > 0$, but an analytical continuation can be found by considering the contour integral, where the contour goes out along the real axis, makes a quarter circle to either the positive or negative imaginary axis and goes back to zero. By letting the radius of the circle go to infinity, we essentially rotate the line of integration from the real onto the imaginary axis. For the $m = 0$ term in (24.39), we transform $x \to ix$ and the integral takes on the form

$$\int_0^{\infty} dx\, h(x)\, r^x\, e^{ix\sigma} = i\int_0^{\infty} dx\, h(ix)\, r^{ix} e^{-x\sigma}.$$

The integrand is now exponentially decreasing for all $r > 0$ and $\sigma \neq 0$ or 2π. The last condition reminds us again of the existence of a branch cut at $\text{Re } z \geq 1$. By the same technique, we find the analytic continuation for all the other integrals in (24.39). The real axis is then rotated according to $x \to \text{sign}(m)ix$ where $\text{sign}(m)$ refers to the sign of m.

$$\int_0^\infty dx\, e^{\pm 2\pi i|m|x} h(x)\, r^x e^{ix\sigma} = \pm i \int_0^\infty dx\, h(\pm ix)\, r^{\pm ix} e^{-x(2\pi|m|\pm\sigma)}.$$

Changing summation and integration, we can carry out the sum over $|m|$ explicitly and one finally obtains the compact expression

$$
\begin{aligned}
f(z) \;=\;& \frac{1}{2}h(0) + i \int_0^\infty dx\, h(ix)\, r^{ix} e^{-x\sigma} \\
&+\; i \int_0^\infty dx\, \frac{e^{-2\pi x}}{1 - e^{-2\pi x}} \left[h(ix) r^{ix} e^{-x\sigma} - h(-ix) r^{-ix} e^{x\sigma} \right].
\end{aligned}
\tag{24.40}
$$

The transformation from the original sum to the two integrals in (24.40) is exact for $r \leq 1$, and provides an analytic continuation for $r > 0$. The expression (24.40) is especially useful for an efficient numerical calculations of a dynamical zeta function for $|z| > 1$, which is essential when searching for its zeros and poles.

24.3.3 Curvature contributions

So far, we have discussed only the fundamental term $\sum_{n=1}^\infty t_n$ in (24.32), and showed how to deal with such power series with algebraically decreasing coefficients. The fundamental term determines the main structure of the zeta function in terms of the leading order branch cut. Corrections to both the zeros and poles of the dynamical zeta function as well as the leading and subleading order terms in expansions like (24.34) are contained in the curvature terms in (24.32). The first curvature correction is the 2-cycle sum

$$\sum_{m=1}^\infty \sum_{n=1}^\infty \frac{1}{2}(t_{mn} - t_m t_n),$$

with algebraically decaying coefficients which again diverge for $|z| > 1$. The analytically continued curvature terms have as usual branch cuts along the positive real z axis. Our ability to calculate the higher order curvature terms depends on how much we know about the cycle weights t_{mn}. The form of the cycle stability (24.6) suggests that t_{mn} decrease asymptotically as

$$t_{mn} \sim \frac{1}{(nm)^{1+1/s}}
\tag{24.41}$$

for 2-cycles, and in general for n-cycles as

$$t_{m_1 m_2 \ldots m_n} \sim \frac{1}{(m_1 m_2 \ldots m_n)^{1+1/s}}\,.$$

If we happen to know the cycle weights $t_{m_1 m_2 \ldots m_n}$ analytically, we may proceed as in sect. 24.3.2, transform the multiple sums into multiple integrals and rotate the integration contours.

We have reached the edge of what has been accomplished so far in computing and what is worth the dynamical zeta functions from periodic orbit data. In the next section, we describe a probabilistic method applicable to intermittent maps which does not rely on periodic orbits.

### 24.3.4 Stability ordering for intermittent flows

Longer but less unstable cycles can give larger contributions to a cycle expansion than short but highly unstable cycles. In such situations, truncation by length may require an exponentially large number of very unstable cycles before a significant longer cycle is first included in the expansion. This situation is best illustrated by intermittent maps. The simplest of these is the Farey map

$$f(x) = \begin{cases} f_0 = x/(1-x) & 0 \leq x \leq 1/2 \\ f_1 = (1-x)/x & 1/2 \leq x \leq 1 \end{cases}, \qquad .
\tag{24.42}$$

For the Farey map, the symbolic dynamics is of complete binary type, so the lack of shadowing is not due to the lack of a finite grammar, but rather to the intermittency caused by the existence of the marginal fixed point $x_0 = 0$, for which the stability multiplier is $\Lambda_0 = 1$. This fixed point does not participate directly in the dynamics and is omitted from cycle expansions. Its presence is, however, very much felt instead in the stabilities of neighboring cycles with n consecutive iterates of the symbol 0, whose stability falls of only as $\Lambda \sim n^2$, in contrast to the most unstable cycles with n consecutive 1's, which are exponentially unstable, $|\Lambda_{01^n}| \sim [(\sqrt{5}+1)/2]^{2n}$.

The symbolic dynamics is of complete binary type. A quick count in the style of sect. 15.7.2 leads to a total of 74,248,450 prime cycles of length 30 or less, not including the marginal point $x_0 = 0$. Evaluating a cycle expansion to this order is an impressive computational feat. However, stability of the least unstable cycle omitted is roughly $\Lambda_{10^{30}} \sim 30^2 = 900$, so it yields a 0.1% correction. The situation may be much worse than this estimate suggests, because the next 10^{31} cycle contributes a similar amount, and could easily reinforce the error. Adding up all such omitted terms, we arrive at an estimated error of about 3%, for a cycle-length truncated cycle expansion based on more than 10^9 pseudo-cycle terms! On the other hand, if one truncates by stability at $\Lambda_{\text{max}} = 3000$, only 409 prime cycles suffice to attain the same accuracy of about a 3% error, figure 24.8.

Figure 24.8: Comparison of cycle expansion truncation schemes for the Farey map (24.42); the deviation of the truncated cycles expansion for $|1/\zeta_N(0)|$ from the exact flow conservation value $1/\zeta(0) = 0$ is a measure of the accuracy of the truncation. The jagged line is the logarithm of the stability ordering truncation error; the smooth line is smoothed according to sect. 20.6.2; the diamonds indicate the error due to the topological length truncation, with the maximal cycle length N shown. They are placed along the stability cutoff axis at points determined by the condition that the total number of cycles is the same for both truncation schemes.
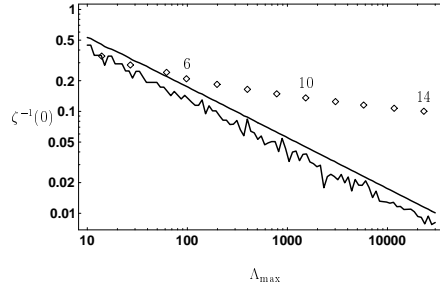
As the Farey map maps the unit interval onto itself, the leading eigenvalue of the Perron-Frobenius operator should equal $s_0 = 0$, so $1/\zeta(0) = 0$. Deviations from this exact result give an indication of the convergence of a given cycle expansion. Errors corresponding to different truncation schemes are indicated in figure 24.8. We see that topological length truncation schemes are hopelessly bad in this case; stability length truncations are somewhat better, but still rather bad. In simple cases like this one, where intermittency is caused by a single marginal fixed point, convergence can be improved by going to infinite alphabets.

24.4 BER zeta functions

So far we have focused on 1-d models as the simplest setting in which to investigate dynamical implications of marginal fixed points. We now take an altogether different track and describe how probabilistic methods may be employed in order to write down approximate dynamical zeta functions for intermittent systems.

We will discuss the method in a very general setting, for a flow in arbitrary dimension. The key idea is to introduce a surface of section $\mathcal{P}$ such that all trajectories traversing this section will have spent some time both near the marginal stable fixed point and in the chaotic phase. An important quantity in what follows is (3.5), the *first return time* $\tau(x)$, or the time of flight of a trajectory starting in x to the next return to the surface of section $\mathcal{P}$. The period of a periodic orbit p intersecting the $\mathcal{P}$ section n_p times is

$$T_p = \sum_{k=0}^{n_p-1} \tau(f^k(x_p)),$$

where $f(x)$ is the Poincaré map, and $x_p \in \mathcal{P}$ is a periodic point. The dynamical

zeta function (19.15)

$$1/\zeta(z, s, \beta) = \prod_p \left(1 - \frac{z^{n_p} e^{\beta A_p - s T_p}}{|\Lambda_p|}\right), \qquad A_p = \sum_{k=0}^{n_p-1} a(f^k(x_p)), \qquad (24.43)$$

chapter 17

associated with the observable $a(x)$ captures the dynamics of both the flow *and* the Poincaré map. The dynamical zeta function for the flow is obtained as $1/\zeta(s, \beta) = 1/\zeta(1, s, \beta)$, and the dynamical zeta function for the discrete time Poincaré map is $1/\zeta(z, \beta) = 1/\zeta(z, 0, \beta)$.

Our basic assumption will be *probabilistic*. We assume that the chaotic interludes render the consecutive *return* (or *recurrence*) times $T(x_i)$, $T(x_{i+1})$ and observables $a(x_i)$, $a(x_{i+1})$ effectively uncorrelated. Consider the quantity $e^{\beta A(x_0,n) - sT(x_0,n)}$ averaged over the surface of section $\mathcal{P}$. With the above probabilistic assumption the large n behavior is

$$\langle e^{\beta A(x_0,n) - sT(x_0,n)} \rangle_{\mathcal{P}} \sim \left(\int_{\mathcal{P}} e^{\beta a(x) - s\tau} \rho(x) dx\right)^n,$$

where $\rho(x)$ is the invariant density of the Poincaré map. This type of behavior is equivalent to there being only one zero $z_0(s, \beta) = \int e^{\beta a(x) - s\tau(x)} \rho(x) dx$ of $1/\zeta(z, s, \beta)$ in the z-β plane. In the language of Ruelle-Pollicott resonances this means that there is an infinite gap to the first resonance. This in turn implies that $1/\zeta(z, s, \beta)$ may be written as

remark 17.1

$$1/\zeta(z, s, \beta) = z - \int_{\mathcal{P}} e^{\beta a(x) - s\tau(x)} \rho(x) dx, \qquad (24.44)$$

where we have neglected a possible analytic and non-zero prefactor. The dynamical zeta function of the flow is now

$$1/\zeta(s, \beta) = 1/\zeta(1, s, \beta) = 1 - \int_{\mathcal{P}} e^{\beta a(x)} \rho(x) e^{-s\tau(x)} dx. \qquad (24.45)$$

Normally, the best one can hope for is a finite gap to the leading resonance of the Poincaré map. with the above dynamical zeta function only approximatively valid. As it is derived from an approximation due to Baladi, Eckmann, and Ruelle, we shall refer to it as the BER zeta function $1/\zeta_{\text{BER}}(s, \beta)$ in what follows.

A central role is played by the probability distribution of return times

$$\psi(\tau) = \int_{\mathcal{P}} \delta(\tau - \tau(x)) \rho(x) dx \qquad (24.46)$$

exercise 25.6

The BER zeta function at $\beta = 0$ is then given in terms of the Laplace transform of this distribution

$$1/\zeta_{\text{BER}}(s) = 1 - \int_0^\infty \psi(\tau)e^{-s\tau}d\tau.$$

Example 24.1 *Return times for the Bernoulli map.*   *For the Bernoulli shift map (23.6)*

$$x \mapsto f(x) = 2x \bmod 1,$$

one easily derives the distribution of return times

$$\psi_n = \frac{1}{2^n} \qquad n \geq 1.$$

The BER zeta function becomes (by the discrete Laplace transform (18.9))

$$
\begin{aligned}
1/\zeta_{\text{BER}}(z) &= 1 - \sum_{n=1}^\infty \psi_n z^n = 1 - \sum_{n=1}^\infty \frac{z^n}{2^n} \\
&= \frac{1-z}{1-z/2} = \zeta^{-1}(z)/(1 - z/\Lambda_0).
\end{aligned}
\tag{24.47}
$$

Thanks to the uniformity of the piecewise linear map measure (16.13) the "approximate" zeta function is in this case the exact *dynamical zeta function, with the periodic point $\overline{0}$ pruned.*

Example 24.2 *Return times for the model of sect. 24.2.1.*   *For the toy model of sect. 24.2.1 one gets $\psi_1 = |\mathcal{M}_1|$, and $\psi_n = |\mathcal{M}_n|(1-b)/(1-a)$, for $n \geq 2$, leading to a BER zeta function*

$$1/\zeta_{\text{BER}}(z) = 1 - z|\mathcal{M}_1| - \sum_{n=2}^\infty |\mathcal{M}_n|z^n,$$

which again coincides with the exact result, (24.11).

It may seem surprising that the BER approximation produces exact results in the two examples above. The reason for this peculiarity is that both these systems are piecewise linear and have complete Markov partitions. As long as the map is piecewise linear and complete, and the probabilistic approximation is exactly fulfilled, the cycle expansion curvature terms vanish. The BER zeta function and the fundamental part of a cycle expansion discussed in sect. 20.1.1 are indeed intricately related, but not identical in general. In particular, note that the BER zeta function obeys the flow conservation sum rule (20.17) by construction, whereas the fundamental part of a cycle expansion as a rule does not.

Résumé

The presence of marginally stable fixed points and cycles changes the analytic structure of dynamical zeta functions and the rules for constructing cycle expansions. The marginal orbits have to be omitted, and the cycle expansions now need to include families of infinitely many longer and longer unstable orbits which accumulate toward the marginally stable cycles. Correlations for such non-hyperbolic systems may decay algebraically with the decay rates controlled by the branch cuts of dynamical zeta functions. Compared to pure hyperbolic systems, the physical consequences are drastic: exponential decays are replaced by slow power-law decays, and transport properties, such as the diffusion may become anomalous.

Commentary

Remark 24.1 What about the evolution operator formalism?   The main virtue of evolution operators was their semigroup property (17.18). This was natural for hyperbolic systems where instabilities grow exponentially, and evolution operators capture this behavior due to their multiplicative nature. Whether the evolution operator formalism is a good way to capture the slow, power law instabilities of intermittent dynamics is less clear. The approach taken here leads us to a formulation in terms of *dynamical zeta functions* rather than spectral determinants, circumventing evolution operators altogether. It is not known if the spectral determinants formulation would yield any benefits when applied to intermittent chaos. Some results on spectral determinants and intermittency can be found in [24.2]. A useful mathematical technique to deal with isolated marginally stable fixed point is that of *inducing*, that is, replacing the intermittent map by a completely hyperbolic map with infinite alphabet and redefining the discrete time; we have used this method implicitly by changing from a finite to an infinite alphabet. We refer to refs. [24.3, 24.20] for detailed discussions of this technique, as well as applications to 1-dimensional maps.

Remark 24.2 Intermittency.   Intermittency was discovered by Manneville and Pomeau [24.1] in their study of the Lorenz system. They demonstrated that in neighborhood of parameter value $r_c = 166.07$ the mean duration of the periodic motion scales as $(r - r_c)^{1/2}$. In ref. [24.5] they explained this phenomenon in terms of a 1-dimensional map (such as (24.1)) near tangent bifurcation, and classified possible types of intermittency.

Piecewise linear models like the one considered here have been studied by Gaspard and Wang [24.6]. The escape problem has here been treated following ref. [24.7], resummations following ref. [24.8]. The proof of the bound (24.28) is given in P. Dahlqvist's notes, see `ChaosBook.org/extras/PDahlqvistEscape.pdf`.

Farey map (24.42) has been studied widely in the context of intermittent dynamics, for example in refs. [24.16, 24.17, 20.3, 24.18, 24.19, 20.15, 24.2]. The Fredholm determinant and the dynamical zeta functions for the Farey map (24.42) and the related Gauss shift map (16.47) have been studied by Mayer [24.16]. He relates the continued fraction transformation to the Riemann zeta function, and constructs a Hilbert space on which the

evolution operator is self-adjoint, and its eigenvalues are exponentially spaced, just as for the dynamical zeta functions [24.24] for "Axiom A" hyperbolic systems.

Remark 24.3 Tauberian theorems.   In this chapter we used Tauberian theorems for power series and Laplace transforms: Feller's monograph [24.9] is a highly recommended introduction to these methods.

Remark 24.4 Probabilistic methods, BER zeta functions.   Probabilistic description of intermittent chaos was introduced by Geisal and Thomae [24.10]. The BER approximation studied here is inspired by Baladi, Eckmann and Ruelle [24.14], with further developments in refs. [24.13, 24.15].

Exercises

24.1. **Integral representation of Jonquière functions.** Check the integral representation

$$J(z, \alpha) = \frac{z}{\Gamma(\alpha)} \int_0^\infty d\xi \, \frac{\xi^{\alpha-1}}{e^\xi - z} \quad \text{for} \quad \alpha > 0 . (24.48)$$

Note how the denominator is connected to Bose-Einstein distribution. Compute $J(x + i\epsilon) - J(x - i\epsilon)$ for a real $x > 1$.

24.2. **Power law correction to a power law.**   Expand (24.21) further and derive the leading power law correction to (24.24).

24.3. **Power-law fall off.**   In cycle expansions the stabilities of orbits do not always behave in a geometric fashion. Consider the map f
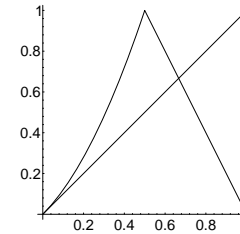
This map behaves as $f \to x$ as $x \to 0$. Define a symbolic dynamics for this map by assigning 0 to the points that land on the interval $[0, 1/2]$ and 1 to the points that land on $(1/2, 1]$. Show that the stability of orbits that spend a long time on the 0 side goes as n^2. In particular, show that

$$\Lambda_{\underbrace{00\cdots 0}_{n} 1} \sim n^2$$

24.4. **Power law fall-off of Floquet multipliers in the stadium billiard**[**].   From the cycle expansions point of view, the most important consequence of the shear in $\mathbf{J}^n$ for long sequences of rotation bounces n_k in (8.13) is that the Λ_n grows only as a power law in number of bounces:

$$\Lambda_n \propto n_k^2 . \qquad (24.49)$$

Check.

24.5. **Probabilistic zeta function for maps.**   Derive the probabilistic zeta function for a map with recurrence distribution ψ_n.

24.6. **Accelerated diffusion.**   Consider a map h, such that $\hat{h} = \hat{f}$, but now running branches are turner into standing branches and vice versa, so that $1, 2, 3, 4$ are standing while 0 leads to both positive and negative jumps. Build the corresponding dynamical zeta function and show that

$$\sigma^2(t) \sim \begin{cases} t & \text{for } \alpha > 2 \\ t \ln t & \text{for } \alpha = 2 \\ t^{3-\alpha} & \text{for } \alpha \in (1, 2) \\ t^2 / \ln t & \text{for } \alpha = 1 \\ t^2 & \text{for } \alpha \in (0, 1) \end{cases}$$

24.7. **Anomalous diffusion (hyperbolic maps).**   Anomalous diffusive properties are associated to deviations from linearity of the variance of the phase variable we are looking at: this means the diffusion constant (17.13) either vanishes or diverges. We briefly illustrate in this exercise how the local local properties of a map are crucial to account for anomalous behavior even for hyperbolic systems.

Consider a class of piecewise linear maps, relevant to the problem of the onset of diffusion, defined by

$$f_\epsilon(x) = \begin{cases} \Lambda x & \text{for } x \in \left[0, x_1^+\right] \\ a - \Lambda_{\epsilon,\gamma}|x - x^+| & \text{for } x \in \left[x_1^+, x_2^+\right] \\ 1 - \Lambda'(x - x_2^+) & \text{for } x \in \left[x_2^+, x_1^-\right] \\ 1 - a + \Lambda_{\epsilon,\gamma}|x - x^-| & \text{for } x \in \left[x_1^-, x_2^-\right] \\ 1 + \Lambda(x - 1) & \text{for } x \in \left[x_2^-, 1\right] \end{cases}$$

where $\Lambda = (1/3 - \epsilon^{1/\gamma})^{-1}$, $\Lambda' = (1/3 - 2\epsilon^{1/\gamma})$, $\Lambda_{\epsilon,\gamma} = \epsilon^{1-1/\gamma}$, $a = 1 + \epsilon$, $x^+ = 1/3$, $x_1^+ = x^+ - \epsilon^{1/\gamma}$, $x_2^+ = x^+ + \epsilon^{1/\gamma}$, and the usual symmetry properties (25.11) are satisfied.

Thus this class of maps is characterized by two escaping windows (through which the diffusion process may take place) of size $2\epsilon^{1/\gamma}$: the exponent γ mimicks the order of the maximum for a continuous map, while piecewise linearity, besides making curvatures vanish and leading to finite cycle expansions, prevents the appearance of stable cycles. The symbolic dynamics is easily described once we consider a sequence of parameter values $\{\epsilon_m\}$, where $\epsilon_m = \Lambda^{-(m+1)}$: we then partition the unit interval though the sequence of points $0, x_1^+, x^+, x_2^+, x_1^-, x^-, x_2^-, 1$ and label the corresponding sub–intervals $1, s_a, s_b, 2, d_b, d_a, 3$: symbolic dynamics is described by an unrestricted grammar over the following set of symbols

$$\{1, 2, 3, s_\# \cdot 1^i, d_\# \cdot 3^k\} \qquad \# = a, b \quad i, k = m, m +$$

This leads to the following dynamical zeta function:

$$\zeta_0^{-1}(z, \alpha) = 1 - \frac{2z}{\Lambda} - \frac{z}{\Lambda'} - 4\cosh(\alpha)\epsilon_m^{1/\gamma-1}\frac{z^{m+1}}{\Lambda^m}\left(1 - \frac{z}{\Lambda}\right)^{-1}$$

from which, by (25.8) we get

$$D = \frac{2\epsilon_m^{1/\gamma-1}\Lambda^{-m}(1 - 1/\Lambda)^{-1}}{1 - \frac{2}{\Lambda} - \frac{1}{\Lambda'} - 4\epsilon_m^{1/\gamma-1}\left(\frac{m+1}{\Lambda^m(1-1/\Lambda)} + \frac{1}{\Lambda^{m+1}(1-1/\Lambda)^2}\right)} \quad (24.51)$$

The main interest in this expression is that it allows exploring how D vanishes in the $\epsilon \mapsto 0$ ($m \mapsto \infty$) limit: as

a matter of fact, from (24.51) we get the asymptotic behavior $D \sim \epsilon^{1/\gamma}$, which shows how the onset of diffusion is governed by the order of the map at its maximum.

Remark 24.5 Onset of diffusion for continuous maps. The zoology of behavior for continuous maps at the onset of diffusion is described in refs. [25.15, 25.16, 24.25]: our treatment for piecewise linear maps was introduced in ref. [24.26].

References

[24.1] P. Manneville and Y. Pomeau, *Phys. Lett.* **75A**, 1 (1979).

[24.2] H.H. Rugh, *Inv. Math.* **135**, 1 (1999).

[24.3] T. Prellberg, *Maps of the interval with indifferent fixed points: thermodynamic formalism and phase transitions*, Ph.D. Thesis, Virginia Polytechnic Institute (1991); T. Prellberg and J. Slawny, "Maps of intervals with indifferent fixed points - thermodynamic formalism and phase transitions," *J. Stat. Phys.* **66**, 503 (1992).

[24.4] T. Prellberg, *Towards a complete determination of the spectrum of a transfer operator associated with intermittency*, *J. Phys. A* **36**, 2455 (2003).

[24.5] Y. Pomeau and P. Manneville, *Commun. Math. Phys.* **74**, 189 (1980).

[24.6] P. Gaspard and X.-J. Wang, *Proc. Natl. Acad. Sci. U.S.A.* **85**, 4591 (1988); X.-J. Wang, *Phys. Rev.* **A40**, 6647 (1989); X.-J. Wang, *Phys. Rev.* **A39**, 3214 (1989).

[24.7] P. Dahlqvist, *Phys. Rev. E* **60**, 6639 (1999).

[24.8] P. Dahlqvist, *J. Phys. A* **30**, L351 (1997).

[24.9] W. Feller, *An introduction to probability theory and applications, Vol. II* (Wiley, New York 1966).

[24.10] T. Geisel and S. Thomae, *Phys. Rev. Lett.* **52**, 1936 (1984).

[24.11] T. Geisel, J. Nierwetberg and A. Zacherl, *Phys. Rev. Lett.* **54**, 616 (1985).

[24.12] R. Artuso, G. Casati and R. Lombardi, *Phys. Rev. Lett.* **71**, 62 (1993).

[24.13] P. Dahlqvist, *Nonlinearity* **8**, 11 (1995).

[24.14] V. Baladi, J.-P. Eckmann and D. Ruelle, *Nonlinearity* **2**, 119 (1989).

[24.15] P. Dahlqvist, *J. Phys. A* **27**, 763 (1994).

[24.16] D.H. Mayer, *Bull. Soc. Math. France* **104**, 195 (1976).

[24.17] D. Mayer and G. Roepstorff, *J. Stat. Phys.* **47**, 149 (1987).

[24.18] D. H. Mayer, *Continued fractions and related transformations*, in ref. [12.2].

[24.19] D. H. Mayer, *The Ruelle-Araki transfer operator in classical statistical mechanics* (Springer-Verlag, Berlin, 1980).

[24.20] S. Isola, *J. Stat. Phys.* **97**, 263 (1999).

[24.21] S. Isola, "On the spectrum of Farey and Gauss maps," `mp-arc 01-280`.

[24.22] B. Fornberg and K.S. Kölbig, *Math. of Computation* **29**, 582 (1975).

[24.23] A. Erdélyi, W. Magnus, F. Oberhettinger and F. G. Tricomi, *Higher transcendental functions, Vol. I* (McGraw-Hill, New York, 1953).

[24.24] D. Ruelle, *Inventiones math.* **34**, 231 (1976)

[24.25] S. Grossmann and H. Fujisaka, *Phys. Rev. A* **26**, 1779 (1982).

[24.26] R. Lombardi, Laurea thesis, Universitá degli studi di Milano (1993).

[24.27] A. Gao, J. Xie, and Y. Lan, Accelerating cycle expansions by dynamical conjugacy, 2011, `arXiv:1106.1045`.